

# **DEVELOPMENT AND CHARACTERIZATION OF UNIDIRECTIONAL ALIGNED MACROPOROUS ALGINATE SCAFFOLD BY IONOTROPIC GELATION USING CALCIUM CHLORIDE**

**A THESIS SUBMITTED IN PARTIAL FULFILLMENT OF THE  
REQUIREMENT FOR THE DEGREE OF  
BACHELOR OF TECHNOLOGY  
IN  
BIOTECHNOLOGY**



Submitted by  
**Warsha Barde**  
**111BT0437**

Under the guidance of  
**Prof. Mukesh Kumar Gupta**  
Dept. of Biotechnology and Medical Engineering  
National Institute of Technology, Rourkela

2015



National Institute of Technology, Rourkela

## **CERTIFICATE**

This is to certify that the thesis entitled “**DEVELOPMENT AND CHARACTERIZATION OF UNIDIRECTIONAL ALIGNED MACROPOROUS ALGINATE SCAFFOLD BY IONOTROPIC GELATION USING CALCIUM CHLORIDE**” submitted by

Ms WARSHA BARDE in partial fulfilment of the requirements for the degree of Bachelor of Technology in BIOTECHNOLOGY embodies the bonafide work done by her in the final semester of her degree under the supervision of the undersigned. The thesis or any part of it has not been submitted earlier to any other University / Institute for the award of any Degree or Diploma.

**Prof. Mukesh Kumar Gupta**

Assistant Professor

Department of Biotechnology and medical engineering

National Institute of Technology, Rourkela

# ACKNOWLEDGEMENT

If words are reflected as symbols of appreciation and token of acknowledgement, then words play the role of thanks to exhibit the deeply embedded feeling of gratitude. I am greatly indebted to, who either through guidance, discussion or providing facilities for the thesis work, have served as a beacon light or crowned my efforts with success. I would really like to take this opportunity to thank my project guide, **Prof. Mukesh Kumar Gupta**, Department of Biotechnology and Medical Engineering, NIT Rourkela, for motivating and guiding me throughout the time. I am sincerely thankful to **Prof. Krishna Pramanik**, Dept. of Biotechnology and Medical Engineering, NIT, Rourkela, for providing the necessary facilities for this work. I gratefully extend my sincere thanks to all faculties and to all teaching and non-teaching staff members of Department of Biotechnology & Medical Engineering, National Institute of Technology Rourkela, Orissa.

I also owe a debt of gratitude to Ms. Srishti Gupta, Mr. Vinay Kumar, Mr. K. Gokulanathana, Mr. Iqbal Hussain, Mr. Praveen Kumar Guttula, Mr. C. Gopalakrishana and Ms Tanushree Patra for all the help and support I got from them. This final year project has brought the best in me and I have given everything to be able to live up to the expectations of all. I would like to express my heartily thanks to my friends Amartya Amitav, Turyansu Subhadarshy, labmates and others in the department for their help and support.

Finally, I would like to express my heartfelt thanks to my parents for their blessings, support and constant encouragement.

Warsha Barde

Biotechnology Engineering.

# CONTENT

<b>SERIAL NO.</b>	<b>CHAPTER NO.</b>	<b>CONTENT</b>	<b>PAGE NO.</b>
1		<b>CERTIFICATE</b>	ii
2		<b>ACKNOWLEDGEMENT</b>	iii
3		<b>LIST OF TABLES</b>	vi
4		<b>LIST OF FIGURES</b>	vii
5		<b>ABSTRACT</b>	viii
6	CHAPTER 1	<b>INTRODUCTION AND LITERATURE REVIEW</b>	1
		1.1 Introduction	2
		1.2 Literature review	4
		1.2.1 Biomimetic approaches for biomaterials	4
		1.2.2 Alginate: General properties	5
		1.2.2.1 Structure and characterization	5
		1.2.2.2 Molecular weight and solubility	7
		1.2.2.3 Biocompatibility	7
		1.2.3 Hydrogel formation by ionotropic gelation	7
7	CHAPTER 2	<b>OBJECTIVE AND WORKPLAN</b>	11
		2.1 Objective	12
		2.2 Work plan	13
8	CHAPTER 3	<b>MATERIALS AND METHODS</b>	14
		3.1 Materials	15
		3.2 Methods	15
		3.2.1 Fabrication of alginate scaffolds with aligned pores	15

	3.2.2 Characterization of alginate scaffolds with aligned pores by simple microscopy	15
	3.2.3 FTIR spectroscopy	16
	3.2.4 Water binding capacity	16
	3.2.5 Disintegration test	17
	3.2.6 Haemo-compatibility	17
9	<b>CHAPTER 4 RESULTS AND DISCUSSION</b>	18
	4.1 Fabrication of alginate scaffolds with aligned pores	19
	4.2 Characterization of alginate scaffolds with aligned pores by simple microscopy	20
	4.3 FTIR spectroscopy	22
	4.4 Water binding capacity	23
	4.5 Disintegration test	25
	4.6 Haemo-compatibility	26
	4.7 Conclusion	28
10	<b>REFERENCES</b>	29

## **LIST OF TABLES**

<b>SERIAL NO.</b>	<b>CONTENT</b>	<b>PAGE NO.</b>
1.	Effect of calcium chloride concentration on pore diameter	21
2	Result of % of haemolysis for various hydrogels	27

## **LIST OF FIGURES**

<b>SERIAL NO.</b>	<b>CONTENT</b>	<b>PAGE NO.</b>
1	Chemical structures of G-block, M-block, and alternating block in alginate.	6
2	Bonding interactions between $\text{Ca}^{2+}$ ions and $-\text{COO}^-$ group in the calcium alginate beads.	6
3	Alginate hydrogels prepared by ionic cross-linking (egg-box model) [38]. Only guluronate blocks participate in the formation of a corrugated egg-box-like structure with interstices in which calcium ions are placed. Copyright 2007, Elsevier Science Ltd., Oxford, UK.	8
4	Sketch of the process of ionotropic gelation of alginate. The scheme on the left was adapted from Wenger (1998)	9
5	Hydrogels made with different concentrations of alginate and calcium chloride.	19
6	Effect of $\text{CaCl}_2$ concentration on pore diameter	20
7	FTIR spectra of 0.5%, 1% and 2% alginate solution with 0.5M, 1M and 2M $\text{CaCl}_2$ solution	22
8	Swelling study of 1% alginate gel with distilled water.	24
9	Swelling study of 1% alginate gel with distilled water, 0.5g NaCl, 1.0g NaCl	24
10	Degradation test for 0.5% alginate gel with different concentrations of Calcium chloride	25
11	Degradation test for 1% alginate gel with different concentrations of Calcium chloride	25
12	Degradation test for 2% alginate gel with different concentrations of Calcium chloride	26

## **ABSTRACT**

Regenerative medicine intends to restore lost functionality by healing tissues defects. For this novel types of biodegradable implants have to be used that first foster healing and later take part in the natural remodeling cycle of the body. Ideally, the implant should mimic the desired tissue. That means that the biomaterial should resemble the extracellular matrix (ECM) which is expressed by specific cells and acts as the biological scaffold of living tissues. In this project alginate is crosslinked by a process called ionotropic gelation using calcium chloride to obtain uniaxial and aligned pores with tubular structures in the micrometer range. The characterization of pores was done using simple microscope and Scanning electron microscopy. The change in pore diameter and density was compared in different concentrations of alginate (0.5%, 1% and 2%) and calcium chloride (0.5M, 1M and 2M). Cross-linking density was studied using swelling and disintegration test while chemical bonding was analyzed using FTIR spectroscopy. These tests showed that calcium divalent ions help in cross linking of poly G units and the subsequent formation of egg-box junction which is the underlying principle for the formation of aligned tubular pores.

**Keywords:** Sodium alginate, calcium chloride, aligned pores, micrometer range, tubular structures.



**CHAPTER 1**  
**INTRODUCTION AND LITERATURE REVIEW**

## 1.1 INTRODUCTION

Tissue and organ failure, as a resultant of injury or other type of impairment, is a major health problem. Treatment options available are transplantation (human or xenotransplantation), surgical repair, artificial prosthetics, mechanical devices, and in some cases, drug therapy. However, major damage to a tissue or organ can neither be repaired nor long-term recovery effected in a truly satisfactory way by these methods.

Although significant progress have been made in medical techniques that reconstruct damaged organs or tissues as a result of an accident, trauma or cancer, transplantation of organs or tissues is still a widely acknowledged therapy to treat patients. The surgical procedure that takes tissues from a patient and transplants them back to the impaired site in the patient's body has often been successful. However, autologous transplantation is restricted because of donor site morbidity and infection or discomfort to patients because of secondary surgery. Alternative tissue sources that are taken from other humans or animals are problematic mainly because of immunogenic responses after implantation and a scarcity of donor organs.

Tissue engineering has emerged as a prospective alternative and complementary solution, whereby tissue and organ failure is repaired by implanting natural, artificial, or semisynthetic tissue and organ mimics that are fully functional from the beginning, or that grow into the required functionality.

Recently, tissue engineering, which applies methods from engineering and life sciences to develop semisynthetic constructs to direct tissue regeneration, has appealed many scientists and surgeons to treat patients in a minimally invasive and less painful way.

The tissue engineering method involves

- Isolation of specific cells through a small biopsy from a patient
- Proliferation of these cells on a three-dimensional biomimetic scaffold under controlled culture conditions
- Delivery of the construct to the desired site in the patient's body
- Directing of new tissue formation into the scaffold that can be degraded over time.

Tissue engineering also allows for unique opportunities to examine aspects of the structure-function relationship linked with new tissue formation in the laboratory and to predict the

scientific outcome of the specific therapeutic treatment. In order to accomplish effective regeneration of impaired organs or tissues based on the tissue engineering concept, several critical elements should be taken into consideration like biomaterial scaffolds that serve as a mechanical support for cell growth, progenitor cells that can be differentiated into specific cell types, and inductive growth factors that can modulate cellular activities.

Hydrogels have been used as scaffolds for tissue engineering strategies because of their similarities with extracellular matrix (ECM), excellent biocompatibility, and intrinsic cellular interaction proficiency. Hydrogels are cross-linked macromolecular networks formed by hydrophilic polymers swollen in water or in biological fluids. After implantation, hydrogel porosity leads to local angiogenesis, which is a key requirement for vascularized tissues. The degree of porosity also has a substantial influence on the mechanical properties, with the compressive strength of the scaffold decreasing as porosity increases [1]. The porosity, pore size, pore interconnectivity and pore architecture and play a significant role in cell survival, growth, propagation, and migration to develop functional hydrogel, and secrete ECM [2,3]. The pore interconnectivity permits cell ingrowth, migration, and nutrient dispersion for cell survival [4-6]. By increasing the pore size the extent of ECM secretion also increases [7]. The average pore size of the hydrogels significantly affects the growth and penetration of cells in the 3D scaffold structure of hydrogels. Without using an intrinsic capillary network, the maximal thickness of engineered tissue is approximately 150–200  $\mu\text{m}$  because of insufficient oxygen and nutrient transport within the deeper compartments of the biomaterial [8]. In addition, mean pore size has been shown to impact the amount of contraction a graft will undergo after implantation [9]. The effect of scaffold pore size on tissue regeneration is highlighted by experiments demonstrating the optimum pore size for neovascularization (500  $\mu\text{m}$ ), fibroblast ingrowth (50–150  $\mu\text{m}$ ), regeneration of adult mammalian skin (200–1250  $\mu\text{m}$ ), regeneration of bone (100–350  $\mu\text{m}$ ), osteoid ingrowth (40–100  $\mu\text{m}$ ) and ingrowth of hepatocytes (20  $\mu\text{m}$ ) [10].

## **1.2 LITERATURE REVIEW**

### **1.2.1 BIOMIMETIC APPROACHES FOR BIOMATERIALS**

In most tissue engineering applications biomaterial plays an important role. For example, biomaterials can be used as a substrate on which cells can adhere and migrate, be implanted with a blend of specific cell types as a cell delivery vehicle, and be utilized as a drug carrier to stimulate specific cellular function in the localized region. The development of biomaterials for tissue engineering has recently focused on the design of biomimetic materials that interact with surrounding tissues by biomolecular recognition. When biomaterials are exposed to biological environments, extracellular matrix (ECM) proteins are non-specifically adsorbed on the surface of biomaterials, thereafter cells ultimately interact with the biomaterial surface through the adsorbed ECM proteins. The design of biomimetic materials is an attempt to make the materials such that they are capable of stimulating specific cellular reactions and directing new tissue formation mediated by specific interactions, which can be manipulated by altering design parameters instead of by non-specifically adsorbed ECM proteins.

The development of biomimetic scaffolds plays an important role in engineering tissue scaffolds by regulating cellular responses. Three dimensional (3D) scaffolds serve as a provisional extracellular matrix (ECM) that provide an environment with a desired mechanical and chemical support for cell growth, migration and tissue regeneration. Scaffolds that imitate the features of natural ECM are perfect for tissue engineering as they direct various cellular behaviors including cell adhesion, migration, differentiation and proliferation,. The structural design, physical features, and biochemical properties of scaffolds play vital roles in regulating cellular functions and subsequent tissue maturation [11].

The closer an artificial scaffold material mimics the pattern the easier it can be involved in the natural healing and remodeling processes, which is why more and more researchers try to establish biomimetic approaches for the development of tissue engineering scaffolds. For many tissue engineering applications different anisotropic materials are needed but biological materials are seldom isotropic. E. g. compact bone displays a honeycomb-like structure with overlapping, cylindrical units (osteons) with the so-called Haversian canal in the center. Scaffolds with parallel and aligned pores, imitating the osteon structure of compact bone can be developed by directed ionotropic gelation of the naturally occurring polysaccharide alginate. The parallel channels can be formed *via* a sol-gel-process when di- or multivalent cations

diffuse into the sol in broad front, resulting in an alginate hydrogel. The pore size and pore alignment of such gels is influenced by the concentration of the starting materials (and the preparation procedure (e.g. temperature, drying process)). The phenomenon was already discovered in the last century but the biomedical potential of alginate scaffolds with parallel aligned pores developed by ionotropic gelation has been explored for osteoblasts, stem cell based tissue engineering, axon guiding or co-culture of vascular and muscle cells only in the past few years [11].

## **1.2.2 ALGINATE: GENERAL PROPERTIES**

Alginate is a naturally occurring anionic polymer usually obtained from brown seaweed, and has been comprehensively investigated and used for many biomedical applications, due to its relatively low cost, biocompatibility, low toxicity, and gelation by addition of divalent cations such as  $\text{Ca}^{2+}$ ,  $\text{Cu}^{2+}$  [12]. Alginate which is commercially available is extracted from brown algae (Phaeophyceae), including *Laminaria hyperborea*, *Laminaria japonica*, *Laminaria digitata*, *Macrocystis pyrifera* and, *Ascophyllum nodosum* [13] by treating with aqueous alkali solutions, like NaOH [14]. The extract is then filtered, and either one of sodium or calcium chloride is added to precipitate alginate. The transformation of alginate salt into alginic acid is done by treatment with dilute HCl. After further purification and transformation, water-soluble sodium alginate powder is obtained [15].

### **1.2.2.1 STRUCTURE AND CHARACTERIZATION**

Alginate is a family of linear copolymers containing blocks of  $\beta$ -D-mannuronate (M) and  $\alpha$ -L-guluronate (G) residues linked by (1, 4) glycosidic bonds. The blocks are composed of consecutive G residues (GGGG), consecutive M residues (MMMM), and alternating M and G residues (GMGMGM)<sup>(15)</sup>.

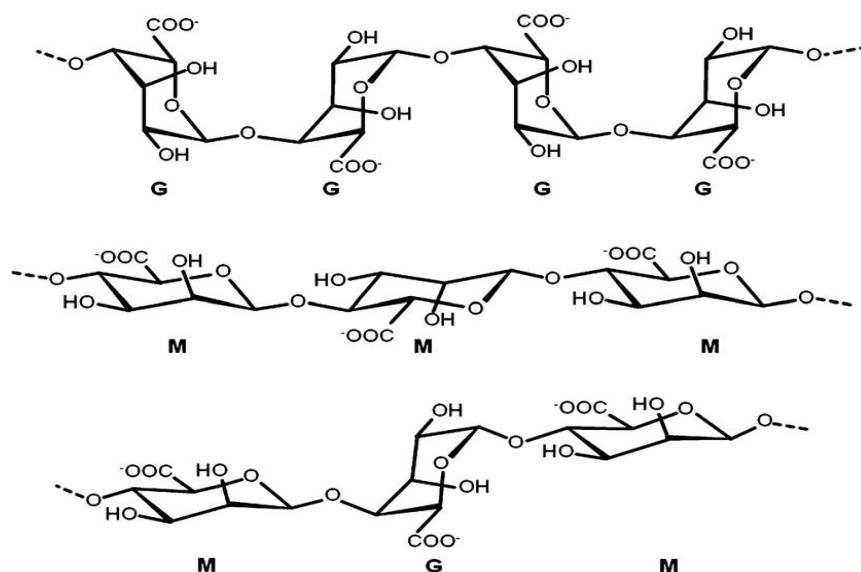


**Fig. 1. Chemical structures of G-block, M-block, and alternating block in alginate.**

Mannuronic (M) and guluronic acid (G) monosaccharide units have identical hydroxyl and carboxylic functional groups but there is difference in their configuration.

Straight MM-sequences do not possess specific sites for binding of cations. Only the G-blocks of alginate are known to participate in intermolecular cross-linking with divalent cations (e.g.,  $\text{Ca}^{2+}$ ) to form hydrogels. The polyguluronate blocks in the alginate molecules form a chelated structure with divalent metal ions, called an egg-box junction with apertures in which the cations pack and can be coordinated [16]. The composition (i.e., M/G ratio), sequence, G-block length and molecular weight are therefore critical factors affecting the physical and chemical properties of alginate and the resulting hydrogels.

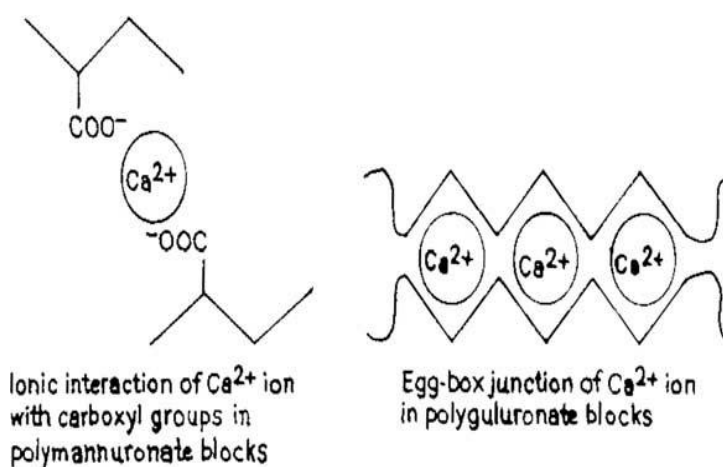


**Fig. 2. Bonding interactions between  $\text{Ca}^{2+}$  ions and  $-\text{COO}^-$  group in the calcium alginate beads.**

### **1.2.2.2 MOLECULAR WEIGHT AND SOLUBILITY**

Commercially available sodium alginates have molecular weights in the range of 32,000 and 400,000 g/mol. The viscosity of alginate solutions increase as pH decreases, and reach a maximum around pH 3–3.5, as carboxylate groups in the alginate backbone become protonated and form hydrogen bonds. Increasing the molecular weight of alginate can result in the improvement of the physical properties of hydrogels. Manipulating the molecular weight and its subsequent distribution can control the pre-gel solution viscosity and post-gelling stiffness. By using a mixture of low and high molecular weight alginate polymers the elastic modulus of gels can be improved considerably, while minimally raising the viscosity of the solution [17].

### **1.2.2.3 BIOCOMPATIBILITY**

Even though the biocompatibility of alginate has been widely evaluated in vivo as well as in vitro, there is still dispute regarding the effect of the alginate composition. Most of this confusion, though, likely relates to erratic levels of purity in the alginate studied in various reports. For example, it has been reported that high M content alginates were immunogenic and approximately 10 times more potent in inducing cytokine production compared with high G alginates [18], but others found little or no immunoresponse around alginate implants [19]. The immunogenic response at the implantation or injection sites might be attributed to impurities remaining in the alginate. Since alginate is obtained from natural sources, various impurities such as heavy metals, proteins, polyphenolic compounds and endotoxins could potentially be present.

### **1.2.3 HYDROGEL FORMATION BY IONOTROPIC GELATION**

Alginate is usually used in the form of a hydrogel in biomedicine, including wound healing, tissue engineering and drug delivery applications. Hydrogels are three-dimensionally cross-linked systems composed of hydrophilic polymers with typically high water content. Chemical and physical cross-linking of hydrophilic polymers are usual approaches to develop hydrogels, and their physic-chemical properties are extremely dependent on the cross-linking type and cross-linking density, besides the chemical composition and molecular weight of the polymers [20].

From an aqueous alginate solution, the most common method to prepare hydrogels is to combine the solution with ionic cross-linking agents, such as divalent cations (i.e.,  $\text{Ca}^{2+}$ ). The divalent cations are thought to bind solely to guluronate units of the alginate chains, as the structure of the guluronate units allows a high degree of coordination of the divalent ions. The guluronate units of one polymer then form junctions with the guluronate blocks of adjacent polymer chains in what is termed the egg-box model of cross-linking, resulting in a gel structure.

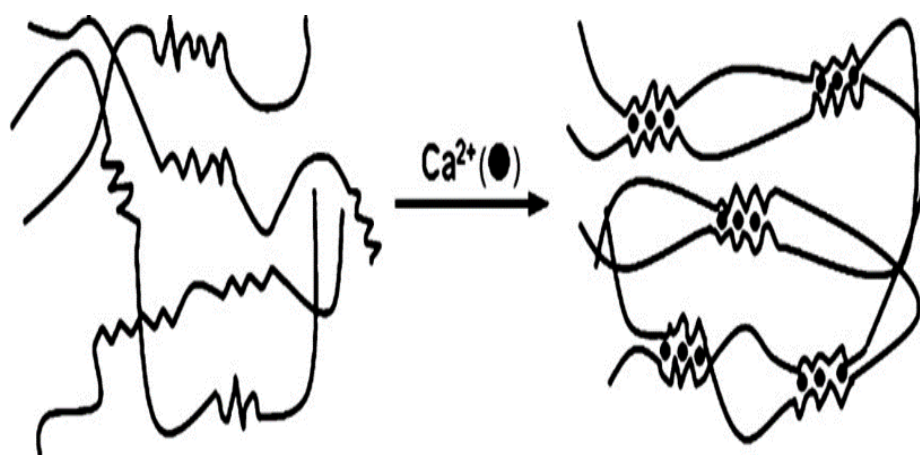


**Fig. 3. Alginate hydrogels prepared by ionic cross-linking (egg-box model) [38]. Only guluronate blocks participate in the formation of a corrugated egg-box-like structure with interstices in which calcium ions are placed. Copyright 2007, Elsevier Science Ltd., Oxford, UK.**

When an alginate sol comes into contact with electrolytes, the molecules start to gel immediately by covering the sol with a dense skin or membrane which is selectively permeable for divalent ions. Microbeads can be produced by dropping small volumes of alginate solution into electrolyte solutions whereas the skin is trapping the sol which gets radially transformed into a gel by the diffusing ions. Anisotropic gels with channel-like pores develop when cations diffuse in broad front from one direction into an alginate sol whereas the saccharide molecules get arranged and cross-linked. Together with the gelation parallel aligned, channel-like pores are formed which can run through the whole length of the gel.



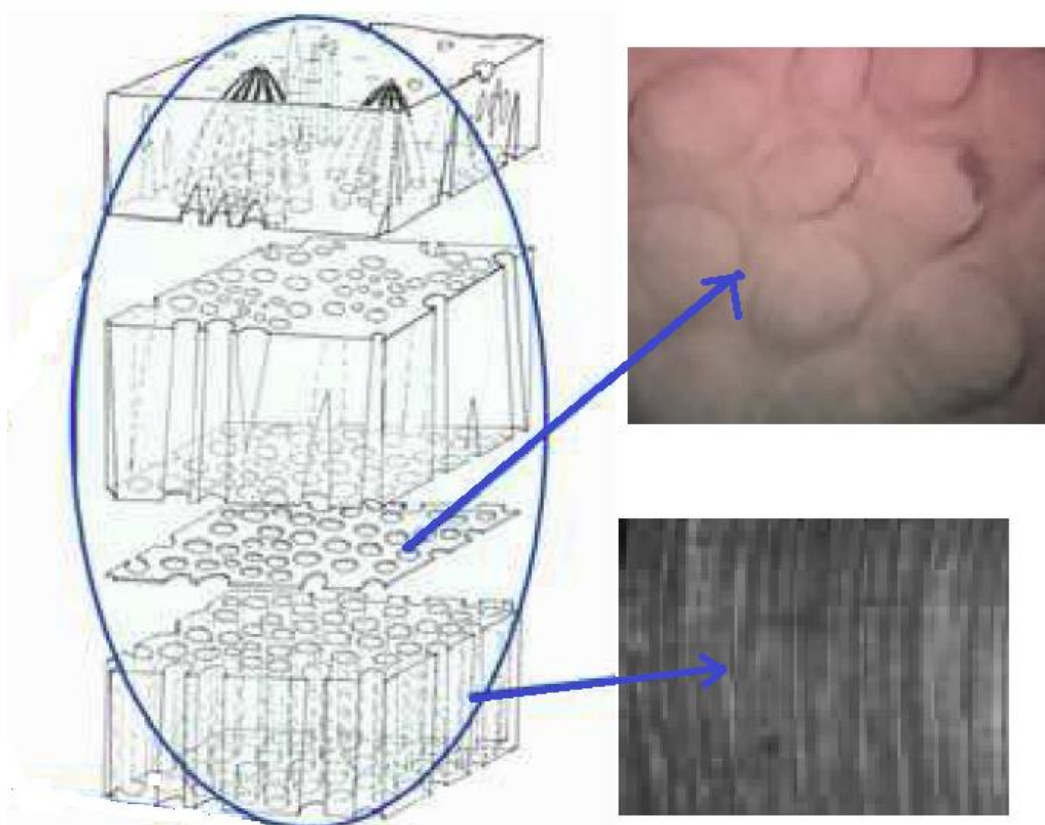


**Fig. 4. Sketch of the process of ionotropic gelation of alginate. The scheme on the left was adapted from Wenger (1998)**

Calcium chloride ( $\text{CaCl}_2$ ) is one of the most commonly used electrolyte to ionically cross-link alginate. However, it typically results in rapid and poorly controlled gelation because of its high solubility in aqueous solutions. The gelation rate is an important factor in controlling gel strength and uniformity when using divalent cations, and slower gelation results in more uniform structures and better mechanical integrity [21]. The gelation temperature also affects gelation rate, and the resultant mechanical properties of the hydrogels. At lower temperatures, the reactivity of ionic cross-linkers (e.g.,  $\text{Ca}^{2+}$ ) is slightly reduced, and cross-linking becomes comparatively slower. The resultant cross-linked gel structure has greater order, leading to enhanced and improved mechanical properties [22]. Moreover, the mechanical properties of ionically cross-linked alginate hydrogels can vary considerably depending on the chemical structure of alginate. For example, hydrogels developed from alginate with a high content of G residues show higher stiffness than those with a low content of G residues [23]. One acute drawback of ionically cross-linked alginate hydrogels is the limited long-term stability in physiological conditions, because these gels dissolve due to release of divalent ions into the surrounding media due to exchange reactions with monovalent cations.

Alginate hydrogels are prepared by various cross-linking methods, and their structural resemblance to extracellular matrices of living tissues permits wide range applications in wound healing, delivery of bioactive agents such as proteins and small chemical drugs, and cell replacement. Alginate gels are also prospective for cell transplantation in tissue engineering. Tissue engineering targets to provide artificial tissue and organ replacements to patients who suffer the loss or failure of an organ or tissue [24]. In this approach, hydrogels are used to deliver cells to the preferred site, provide a space for fresh tissue development, and control the structure and function of the engineered tissue [25].

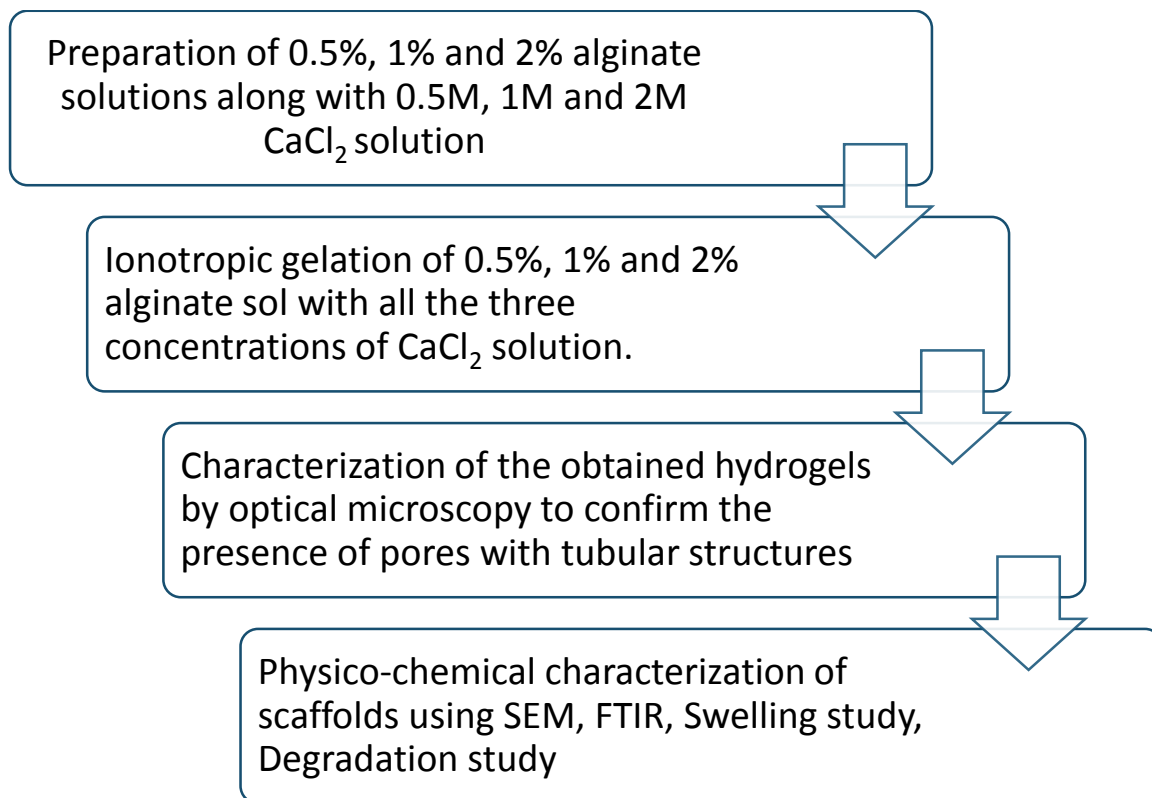
## **CHAPTER 2**

### **OBJECTIVES AND WORK PLAN**

## **2.1 OBJECTIVES**

- Preparation of calcium alginate hydrogel with aligned tubular macro size pores
- Physico-chemical characterization of scaffold
- Potential application of the scaffold in drug delivery and tissue engineering

## 2.2 WORK PLAN



**CHAPTER 3**  
**MATERIALS AND METHODS**

### **3.1 MATERIALS**

Sodium alginate was bought from HIMEDIA.

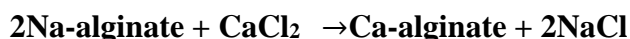
Calcium chloride dihydrate with molecular mass 147g was purchased from HIMEDIA.

Kim Wipes with dimensions 11×21cm were purchased from KIMTECH.

### **3.2 METHODS**

#### **3.2.1 FABRICATION OF ALGINATE SCAFFOLDS WITH ALIGNED PORES**

0.5%, 1% and 2% sodium alginate solution was made along with 0.5M, 1M and 2M calcium chloride solution. Inner walls and bottom of Petri dish was coated with a thin layer of sodium alginate twice and was left to dry. 10ml of sodium alginate solution was poured into the alginate coated petridish. A small piece of Kim Wipe was placed over the petridish and approximately 3-4ml of CaCl<sub>2</sub> was poured over it. After waiting 10-15 minutes a thin alginate gel layer was formed on top of the sodium alginate solution. In the contact zone a primary membrane of gelled alginate with function of selective membrane occurred which only allowed Ca<sup>2+</sup> ions to permeate and not alginate sol. The petridish was then transferred into a tank filled with CaCl<sub>2</sub> solution and was incubated for 24 hours at room temperature to complete gelation.



The gel was then subsequently washed in deionized water to remove unbound Ca<sup>2+</sup> ions.

#### **3.2.2 CHARACTERIZATION OF ALGINATE SCAFFOLDS WITH ALIGNED PORES BY MICROSCOPY**

Thin sections of gel were cut and cross section and longitudinal sections were viewed under simple microscope at 10X magnification.

### 3.2.3 IR SPECTRA

The range of Infrared region is  $12800 \sim 10 \text{ cm}^{-1}$  and can be divided into near-infrared region ( $12800 \sim 4000 \text{ cm}^{-1}$ ), mid-infrared region ( $4000 \sim 200 \text{ cm}^{-1}$ ) and far-infrared region ( $50 \sim 1000 \text{ cm}^{-1}$ ). Infrared spectrum is molecular vibrational spectrum. When exposed to infrared radiation, sample molecules selectively absorb radiation of specific wavelengths which causes the change of dipole moment of sample molecules. Consequently, the vibrational energy levels of sample molecules transfer from ground state to excited state. The frequency of the absorption peak is determined by the vibrational energy gap. The number of absorption peaks is related to the number of vibrational freedom of the molecule. The intensity of absorption peaks is related to the change of dipole moment and the possibility of the transition of energy levels. Therefore, by analyzing the infrared spectrum, one can readily obtain abundant structure information of a molecule. The common used region for infrared absorption spectroscopy is  $4000 \sim 400 \text{ cm}^{-1}$  because the absorption radiation of most organic compounds and inorganic ions is within this region. The alginate IR spectrum (Fig. 2) shows the characteristics peaks at  $3383 \text{ cm}^{-1}$  (OH stretching),  $1607 \text{ cm}^{-1}$  (COOH stretching) and  $1036 \text{ cm}^{-1}$  (C–O–C stretching).

### 3.2.4 WATER BINDING CAPACITY

The alginate gel was cut into pieces of  $1\text{cm} \times 1\text{cm}$  and pre-weighed. These were then immersed in water at  $30^\circ\text{C}$  and their weight change was monitored at different time intervals till the gel pieces showed complete dissolution. The fractional weight change was calculated using the following empirical relationship

$$\text{Dynamic weight change \%} = (\text{Final weight} - \text{Initial weight}) / \text{Initial weight} \times 100$$

The same experiment was repeated by using 0.5g NaCl and 1.0g NaCl dissolved in 100ml of water.

The measurements were made in triplicate and average data was used for calculations. In the various curves plotted, the complete dissolution of beads has been indicated by 100% weight change.



### 3.2.5 DISINTEGRATION TEST

The alginate gel was cut into pieces of 1cm×1cm and pre weighed. These were then stored under phosphate buffer saline (0.1M and pH 7.4) at 30°C and their weight change was monitored at different time intervals till the gel pieces showed complete dissolution. The fractional weight change was calculated using the following empirical relationship:

$$\text{Dynamic weight change \%} = (\text{Final weight} - \text{Initial weight}) / \text{Initial weight} \times 100$$

The measurements were made in triplicate and average data was used for calculations. In the various curves plotted, the complete dissolution of beads has been indicated by 100% weight change.

### 3.2.6 HAEMO-COMPATIBILITY

The alginate hydrogel samples were cut into pieces of 1cm×1cm and then washed with water continuously for 2-3 times. It was mixed with 0.5 ml of EDTA added goat blood diluted with normal saline (prepared in 4:5 ratio), followed by the addition of normal saline (9.5 ml). The positive control (+ve) was prepared by adding 0.5 ml of 0.1 N hydrochloric acid to 0.5 ml of diluted blood. The negative control (-ve) was prepared by adding 0.5 ml of saline to 0.5 ml of diluted blood. The final volume was made up to 10 ml using saline. The positive control and the -ve control were incubated at 37 C for 1 h. After incubation, the samples were subsequently centrifuged at 3000 rpm for 10 min. The supernatant was analyzed at 545 nm using a UV-visible spectrophotometer (UV 3200 double beam, Lab India). The percentage of haemolysis was calculated from the following equation:

$$\% \text{ HAEMOLYSIS} = ( \text{O.D}_{\text{SAMPLE}} - \text{O.D}_{\text{-VE}} / \text{O.D}_{\text{+VE}} - \text{O.D}_{\text{-VE}} ) * 100$$

where,

$\text{O.D}_{\text{SAMPLE}}$  = O.D of sample

$\text{O.D}_{\text{-VE}}$  = O.D of negative control

$\text{O.D}_{\text{+VE}}$  = O.D of positive control

**CHAPTER 4**  
**RESULTS AND DISCUSSION**

## 4.1 FABRICATION OF ALGINATE HYDROGEL

9 hydrogels were made by using 0.5% alginate solution with 0.5M, 1M and 2M  $\text{CaCl}_2$  solution; 1% alginate with 0.5M, 1M and 2M  $\text{CaCl}_2$  and 2% alginate solution with 0.5M, 1M and 2M  $\text{CaCl}_2$  solution.

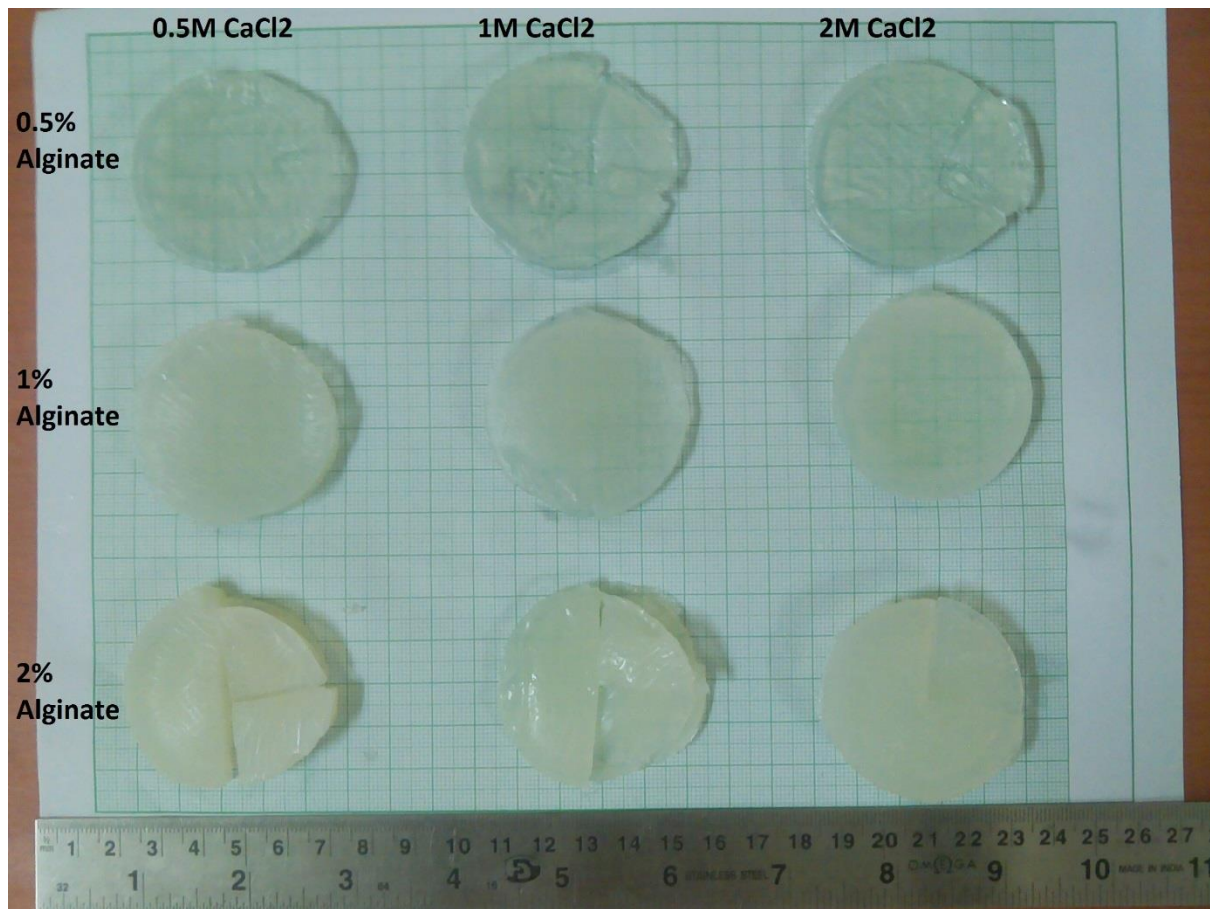


**Fig. 5.**Hydrogels made with different concentrations of alginate and calcium chloride.

As the concentration of alginate in the hydrogel increases, the opacity of hydrogel increases with 0.5% alginate hydrogel being the most transparent and 2% alginate being the most opaque.

## 4.2 MICROGRAPHS OBTAINED FROM SIMPLE MICROSCOPY

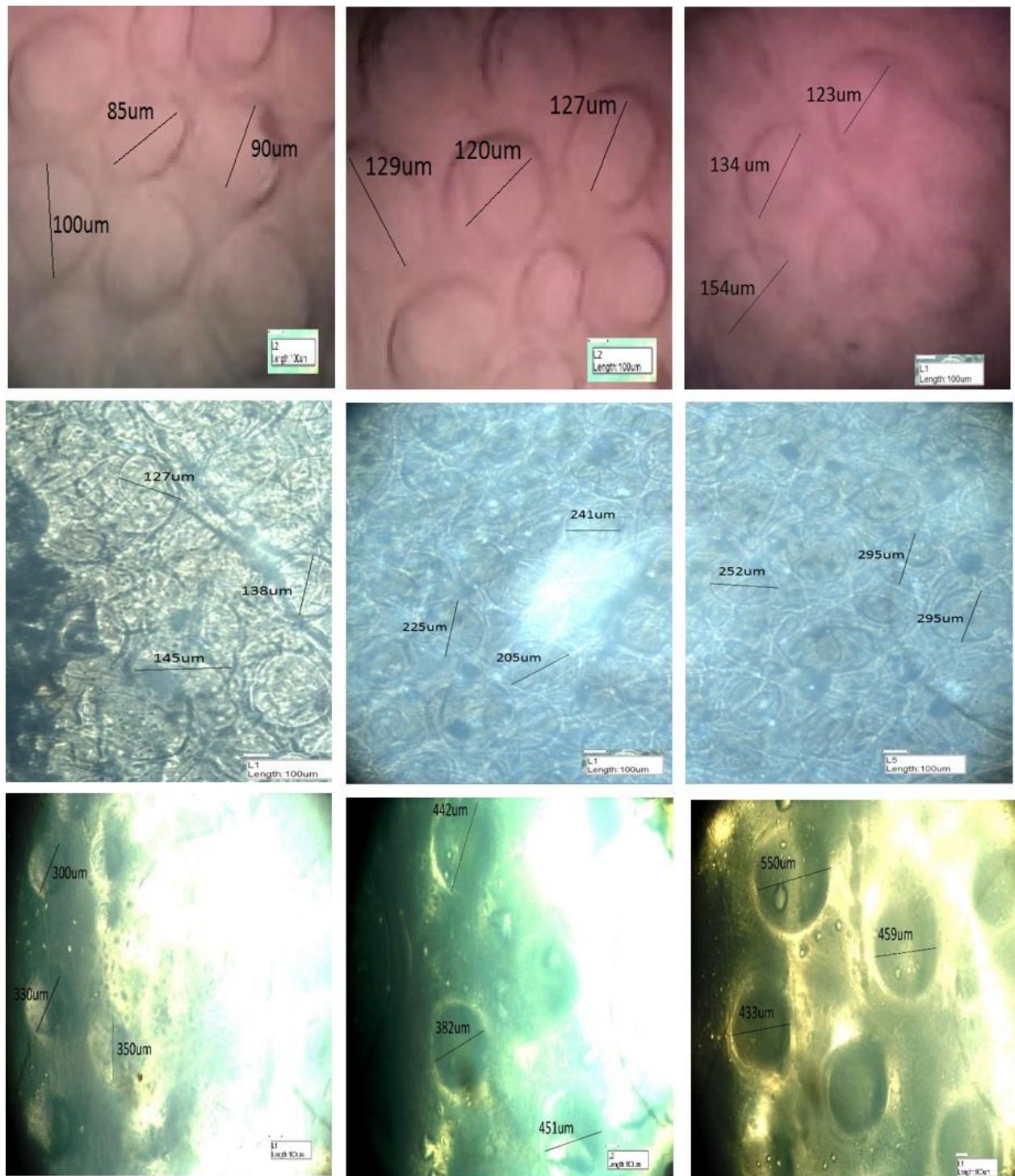


**Fig. 6 Effect of  $\text{CaCl}_2$  concentration on pore diameter**

As the concentration of  $\text{CaCl}_2$  increases, more number of  $\text{Ca}^{2+}$  ions interact with alginate and hence the cross-linking density increases. The pore diameter was calculated using ImageJ and is tabulated in the following table:

**Table 1: Effect of calcium chloride concentration on pore diameter**

CONCENTRATION OF ALGINATE (wt/vol %)	CONCENTRATION OF CALCIUM CHLORIDE SOLUTION (M)	PORE DIAMETER
0.5	0.5	91±7
	1	125±4.7
	2	137±15.7
1.0	0.5	136±9
	1	223±18
	2	280±24.8
2.0	0.5	326±25
	1	425±57
	2	480±61

### 4.3 IR SPECTRA

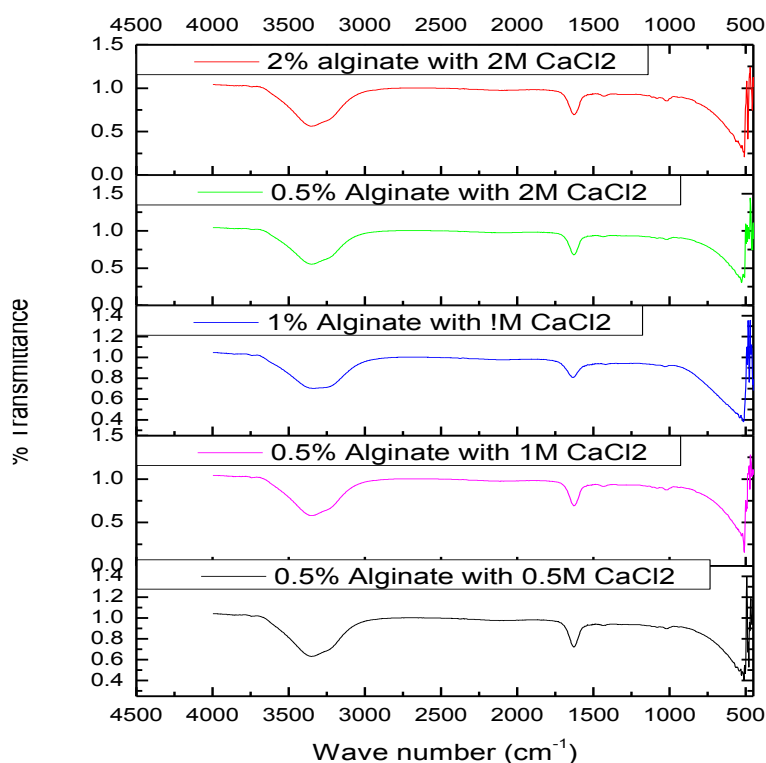


**Fig.7. FTIR spectra of 0.5%, 1% and 2% alginate solution with 0.5M, 1M and 2M CaCl<sub>2</sub> solution**

The alginate FTIR spectrum shows the characteristic peaks at 3242 cm<sup>-1</sup> (OH<sup>-</sup> stretching) (Lawrie, 2007), 1596 and 1407 cm<sup>-1</sup> (COO<sup>-</sup> asymmetric and symmetric stretching), 1081-1024 cm<sup>-1</sup> (C-O-C antisymmetric stretching), and carboxyl and carboxylate at about 1000 to 1400 cm<sup>-1</sup> (Mayur, 2005).

In FTIR spectra of calcium alginate the asymmetric band of carboxylate ion has shifted to lower frequencies from 1596 cm<sup>-1</sup> to 1606 cm<sup>-1</sup>, and the hydroxyl band of sodium alginate has shifted from 3242 cm<sup>-1</sup> to 3337 cm<sup>-1</sup>, because of the interaction of sodium alginate and CaCl<sub>2</sub> (Lawrie, 2007).

#### 4.4 SWELLING STUDY

Swelling study of 1% alginate hydrogel was done with distilled water. The gels showed no increase in weight, i.e. no water uptake. Rather the gels started disintegrating and completely lost their weight after 48 hours which is shown by Fig .8.

When the swelling study was conducted by using 0.5g and 1.0g NaCl in 100ml distilled water, the hydrogels showed water uptake. It is the ionexchange process between  $\text{Na}^+$  and  $\text{Ca}^{2+}$  ions, which is supposed to be responsible for the swelling and subsequent degradation of the beads. The results, as depicted in the Fig. 9, reveal that gels do not show any tendency to take up water and swell in pure distilled water (not containing NaCl). Moreover they begin to lose their weight slightly i.e. by 40% in 6 h and then do not show any tendency to further lose their weight for next 36 h. However, behavior of gels is totally different in distilled water containing 0.5 and 1.0 g NaCl. The gels dipped in pure distilled water do not show any tendency to take up water because no sodium ions are available in the medium which could undergo ion-exchange process with  $\text{Ca}^{2+}$  ions present within the gels. In addition to this, the gels are highly cross-linked and hence do not show any tendency to absorb water and swell. This explains why the gels did not swell in pure distilled water. In the later stage, slight weight loss in gels may be due to the little dissolution of polymannuronate blocks and hence may result in weight loss. The situation is very different with gels which were immersed in the distilled water, containing 0.5 and 1.0 g of NaCl per 100 ml of solvent. Here, there starts ion-exchange process between  $\text{Na}^+$  ions and  $\text{Ca}^{2+}$  ions which are in the polymannuronate blocks. Now since the  $\text{Na}^+$  ions are not able to sufficiently bind the  $-\text{COO}^-$  ion groups in polymannuronate sequences the extent of crosslinking decreases and hence water uptake increases. However after nearly 3 h when most of the  $\text{Ca}^{2+}$  ions present in the poly(M) blocks have been exchanged with  $\text{Na}^+$  ions the ion-exchange process between  $\text{Na}^+$  ions and  $\text{Ca}^{2+}$  ions present in polyguluronate blocks begins. This results in loosening of egg-box structure and thus permit great amount of water to enter. This may be the probable cause of drastic increase in water uptake by the beads after nearly 3 h. After the attainment of equilibrium water uptake, the highly hydrated egg-box structure begins to disintegrate and hence the beads start to lose their weight.



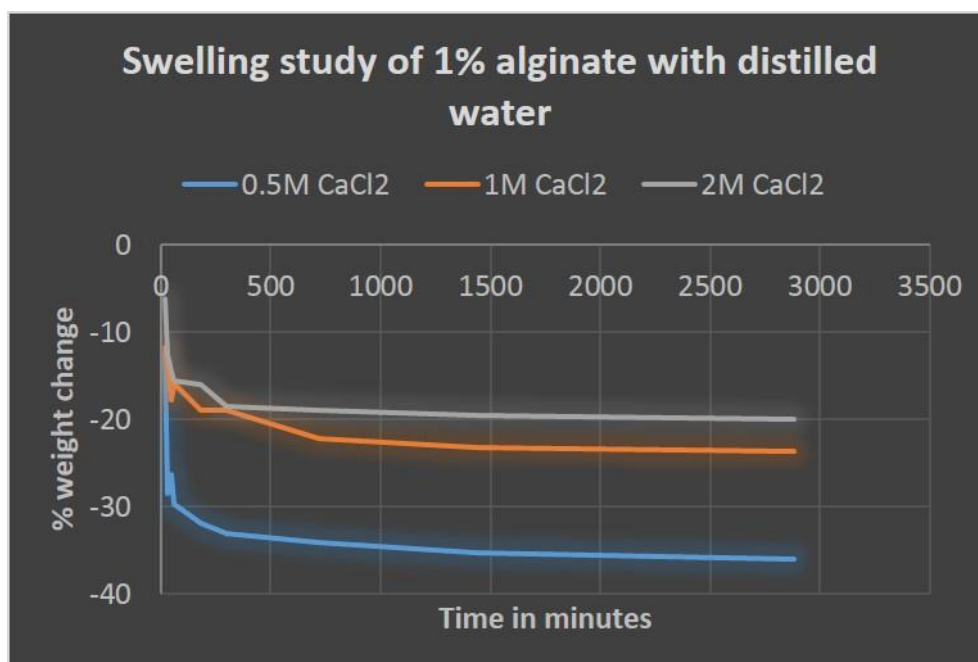


**Fig.8. Swelling study of 1% alginate gel with distilled water.**

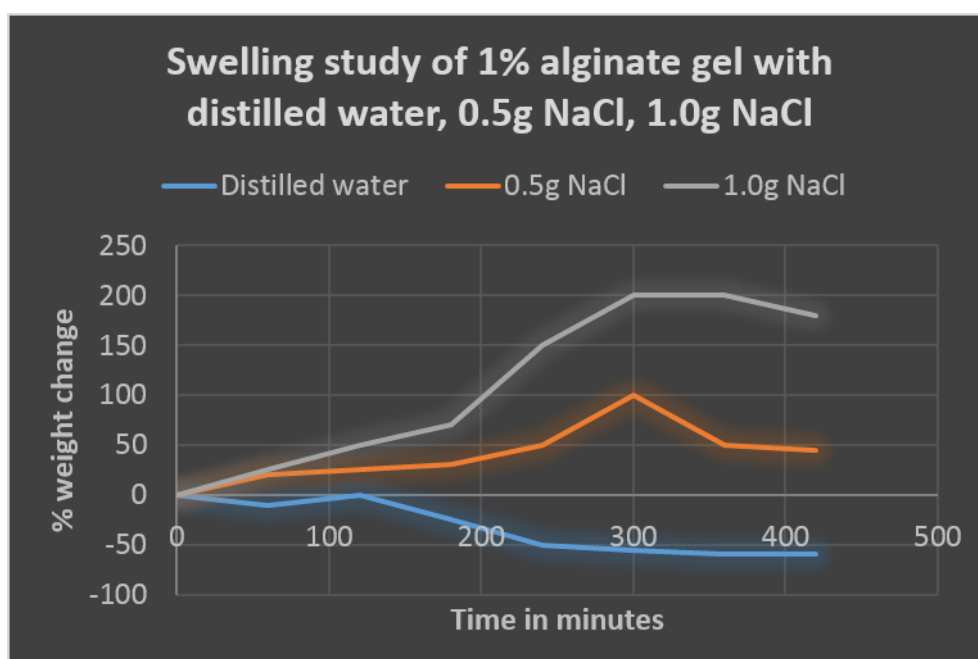


**Fig.9. Swelling study of 1% alginate gel with distilled water, 0.5g NaCl, 1.0g NaCl**



## 4.5 DISINTEGRATION TEST

Degradation study was carried out with all the three concentrations of alginate gel, i.e., 0.5%, 1% and 2%.

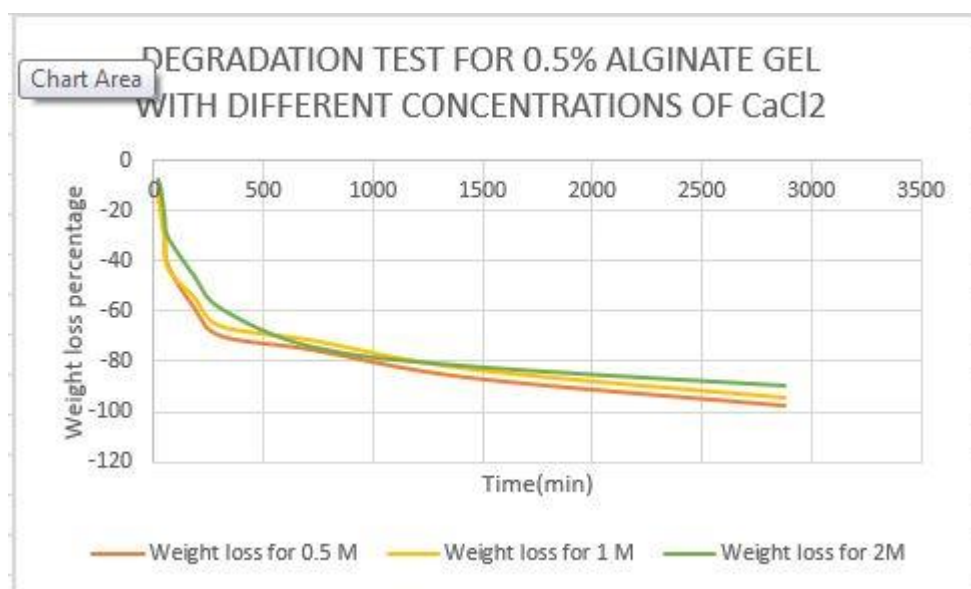


**Fig.10. Degradation test for 0.5% alginate gel with different concentrations of Calcium chloride**

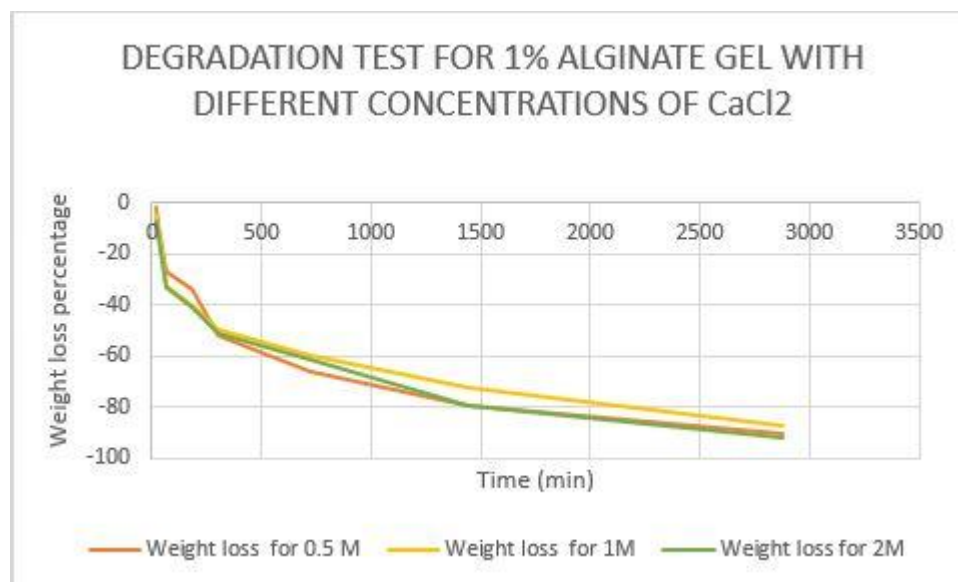


**Fig.11. Degradation test for 1% alginate gel with different concentrations of Calcium chloride**

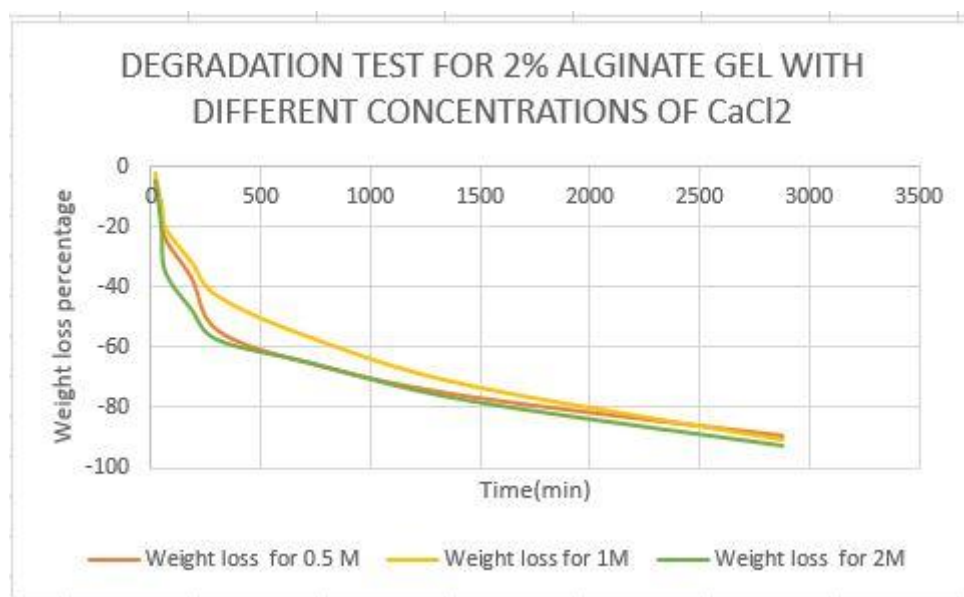


**Fig.12. Degradation test for 2% alginate gel with different concentrations of Calcium chloride**

As is evident from the graph the hydrogel disintegrated completely after 48 hours. In the later stage of swelling process, the  $\text{Ca}^{2+}$  ions which are binding with  $-\text{COO}^-$  group of the polyguluronate units and thus form the tight egg-box structure start to diffuse in the buffer medium. This causes reduction in the cross-linking density. Therefore, the gel starts to lose their weight and finally dissolve. It is also clear that as the extent of crosslinking increases, the maximum water uptake decreases.

## 4.6 HEMOCOMPATIBILITY TEST

Absence of haemolysis is a sign of good haemo-compatibility. The % haemolysis indicates the extent of lysis of red blood cells when kept in contact with the gel. The % haemolysis of all the 4 samples were calculated by the % haemolysis formula and tabulated in Table 2. It was observed that all the 4 samples shown % haemolysis value less than 5 (standard ASTM value) this suggests high haemo-compatibility.

**Table 2: Result of % of haemolysis for various hydrogels**

<b>SERIAL NO</b>	<b>SAMPLE</b>	<b>O.D OF SAMPLE</b>	<b>O.D OF NEGATIVE CONTROL</b>	<b>O.D OF POSITIVE CONTROL</b>	<b>% HEMOLYSIS</b>
<b>1</b>	<b>0.5% alginate with 0.5M CaCl<sub>2</sub></b>	0.108	0.104	0.324	1.8
<b>2</b>	<b>1 % alginate with 1M CaCl<sub>2</sub></b>	0.107	0.104	0.324	1.3
<b>3</b>	<b>2% alginate with 2M CaCl<sub>2</sub></b>	0.106	0.104	0.324	0.9

## 4.7 CONCLUSION

Macro-porous alginate hydrogels with aligned tubular structures were obtained in the macro range by employing ionotropic gelation method using calcium chloride. The following conclusions were drawn from this study:

- The microscopy studies showed that the pore size was in the macro-range and the pore size increased with increase in concentration of calcium chloride solution.
- Swelling tests showed no water uptake with distilled water while there was significant water uptake with saline water.
- Degradation tests showed complete degradation after 48 hours.
- Evaluation of FTIR spectra showed a little shift because of interaction between sodium alginate and calcium divalent ions.
- Haemo-compatibility study showed that the prepared alginate hydrogel was haemo-compatible.

## **REFERENCES**

1. Gerecht S. Townsend S.A. Pressler H. Zhu H. Nijst C.L. Bruggeman J.P. Nichol J.W. Langer R. A porous photocurable elastomer for cell encapsulation and culture. *Biomaterials*. 2007;28:4826. [[PubMed](#)]
2. Mandal B. Kundu S. Cell proliferation and migration in silk fibroin 3D scaffolds. *Biomaterials*. 2009;30:2956. [[PubMed](#)]
3. Lien S.M. Ko L.Y. Huang T.J. Effect of pore size on ECM secretion and cell growth in gelatin scaffold for articular cartilage tissue engineering. *Acta Biomater*. 2009;5:670. [[PubMed](#)]
4. Peppas N.A. *Hydrogels in Medicine and Pharmacy*. Boca Raton, FL: CRC Press; 1987.
5. Gerecht S. Townsend S.A. Pressler H. Zhu H. Nijst C.L. Bruggeman J.P. Nichol J.W. Langer R. A porous photocurable elastomer for cell encapsulation and culture. *Biomaterials*. 2007;28:4826. [[PubMed](#)]
6. Martin I. Obradovic B. Treppo S. Grodzinsky A.J. Langer R. Freed L.E. Vunjak-Novakovic G. Modulation of the mechanical properties of tissue engineered cartilage. *Biorheology*. 2000;37:141. [[PubMed](#)]
7. Lien S.M. Ko L.Y. Huang T.J. Effect of pore size on ECM secretion and cell growth in gelatin scaffold for articular cartilage tissue engineering. *Acta Biomater*. 2009;5:670. [[PubMed](#)]
8. Fidkowski C. Kaazempur-Mofrad M.R. Borenstein J. Vacanti J. Langer R. Wang Y. Endothelialized microvasculature based on a biodegradable elastomer. *Tissue Eng*. 2005;11:302. [[PubMed](#)]
9. Yannas I.V. Lee E. Orgill D.P. Skrabut E.M. Murphy G.F. Synthesis and characterization of a model extracellular matrix that induces partial regeneration of adult mammalian skin. *Proc Natl Acad Sci USA*. 1989;86:933. [[PMC free article](#)] [[PubMed](#)]
10. Whang K. Healy K.E. Elenz D.R. Nam E.K. Tsai D.C. Thomas C.H. Nuber G. Glorieux R. Travers R. Sprague S.M. Engineering bone regeneration with bioabsorbable scaffolds with novel microarchitecture. *Tissue Eng*. 1999;5:35. [[PubMed](#)]
11. *Scaffolds for Tissue Engineering: Biological Design, Materials and Fabrication*, NihalEnginVrana LeRoux MA, Guilak F, Setton LA. Compressive and shear

- properties of alginate gel: effects of sodium ions and alginate concentration. *J Biomed Mater Res* 1999;47:46–53.
12. Kong HJ, Smith MK, Mooney DJ. Designing alginate hydrogels to maintain viability of immobilized cells. *Biomaterials* 2003;24:4023–9.
  13. . Langer R. Vacanti J.P. Tissue engineering. *Science*. 1993;260:920. [[PubMed](#)]
  14. Lutolf M.P. Hubbell J.A. Synthetic biomaterials as instructive extracellular microenvironments for morphogenesis in tissue engineering. *Nat Biotechnol*. 2005;23:47. [[PubMed](#)]
  15. . Bach A.D. Stem-Straeter J. Beier J.P. Bannasch H. Stark G.B. Engineering of muscle tissue. *Clin Plast Surg*. 2003;30:589. [[PubMed](#)]
  16. . Bannasch H. Fohn M. Unterberg T. Bach A.D. Weyand B. Stark G.B. Skin tissue engineering. *Clin Plast Surg*. 2003;30:573. [[PubMed](#)]
  17. . Chen R.R. Mooney D.J. Polymeric growth factor delivery strategies for tissue engineering. *Pharm Res*. 2003;20:1103. [[PubMed](#)]
  18. . Hubbell J.A. Tissue and cell engineering. *Curr Opin Biotechnol*. 2004;15:381. [[PubMed](#)]
  19. Langer R. Tirrell D.A. Designing materials for biology and medicine. *Nature*. 2004;428:487. [[PubMed](#)]
  20. Saltzman W.M. Olbricht W.L. Building drug delivery into tissue engineering. *Nat Rev*. 2002;1:177. [[PubMed](#)]
  21. Silva E.A. Mooney D.J. Synthetic extracellular matrices for tissue engineering and regeneration. *Curr Top Dev Biol*. 2004;64:181. [[PubMed](#)]
  22. Novel Biomaterials with Parallel Aligned Pore Channels by Directed Ionotropic Gelation of Alginate: Mimicking the Anisotropic Structure of Bone Tissue, Florian Despang<sup>1</sup>, Rosemarie Ditttrich<sup>2</sup> and Michael Gelinsky<sup>1</sup> *Max Bergmann Center of Biomaterials and Institute for Materials*
  23. [12] Fischer FG, Dörfel H. Die polyuronsäuren der braunalgen- (kohlenhydrate der algen-I). *Z Physiol Chem* 1955;302:186–203.
  24. Langer R, Vacanti JP. Tissue engineering. *Science* 1993;260:920–6.
  25. [6] Lee KY, Mooney DJ. Hydrogels for tissue engineering. *Chem Rev* 2001;101:1869–79.
  26. George M, Abraham TE. Polyionic hydrocolloids for the intestinal delivery of protein drugs. *J Control Release* 2006;114:1–14.

27. K. Park, W.S.W. Sharaby, H. Park, Physical Gels, in: Biodegradable Hydrogels for Drug Delivery, Technomic Publishing, Lancaster, PA, 1993, pp. 99–140.
28. Biomimetic materials for tissue engineering Heungsoo Shin, Seongbong Jo, Antonios G. Mikos
29. Smidsrod O, Skjak-Bræk G. Alginate as immobilization matrix for cells. *Trend Biotechnol* 1990;8:71–8.
30. Clark DE, Green HC. Alginic acid and process of making same. US Patent 2036922; 1936.
31. Rinaudo M. Main properties and current applications of some polysaccharides as biomaterials. *Polym Int* 2008;57:397–430.
32. Kuo CK, Ma PX. Ionically crosslinked alginate hydrogels as scaffolds for tissue engineering: part 1. structure, gelation rate and mechanical properties. *Biomaterials* 2001;22:511–21.
33. Augst AD, Kong HJ, Mooney DJ. Alginate hydrogels as biomaterials. *Macromol Biosci* 2006;6:623–33.
34. Drury JL, Dennis RG, Mooney DJ. The tensile properties of alginate hydrogels. *Biomaterials* 2004;25:3187–99.